PIC Simulations of Particle Acceleration in Relativistic Magnetized Astrophysical Flows

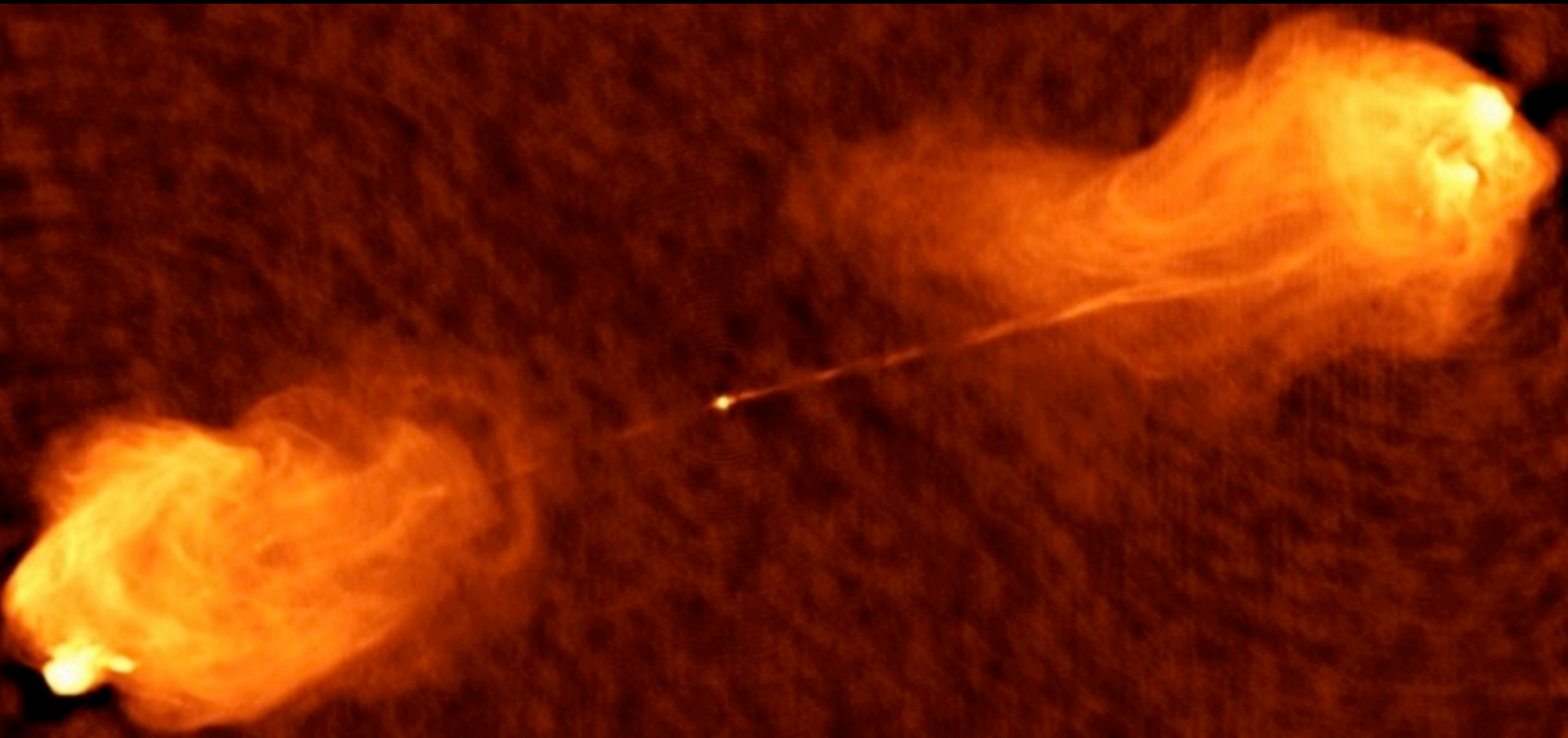

Lorenzo Sironi (ITC-Harvard)
with: A. Spitkovsky, J. Arons, R. Narayan

PCTS Workshop, April 11th 2013

Outline

- Diversity and similarity of relativistic astrophysical flows

- How do microphysical plasma instabilities affect the flow structure, and the particle energy spectrum?

- Particle-in-cell studies of non-thermal particle acceleration:
  - strongly vs weakly magnetized shocks
  - uniform vs alternating fields

- Conclusions and applications

Relativistic flows in astrophysics

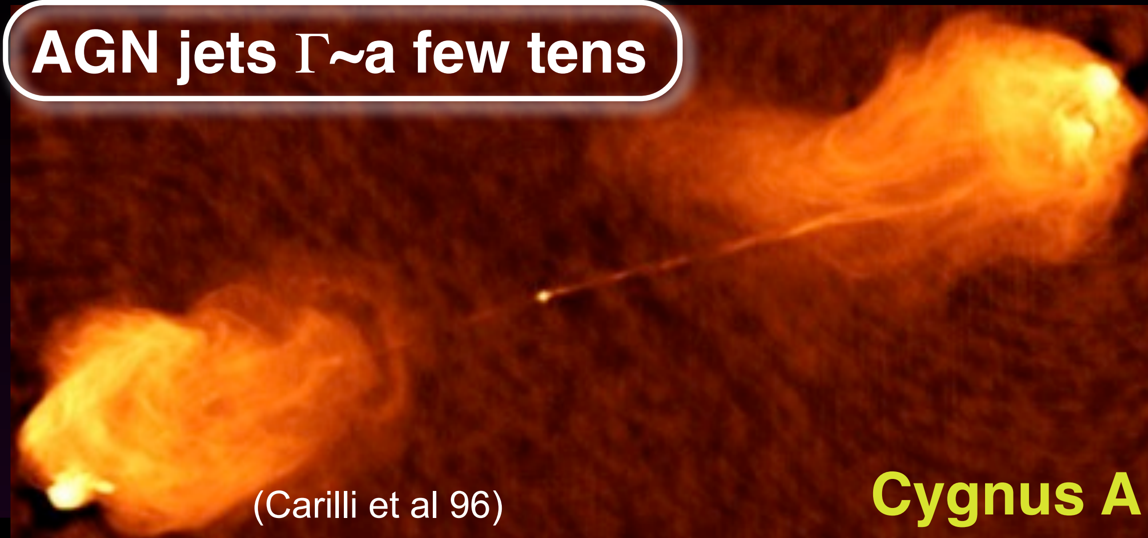

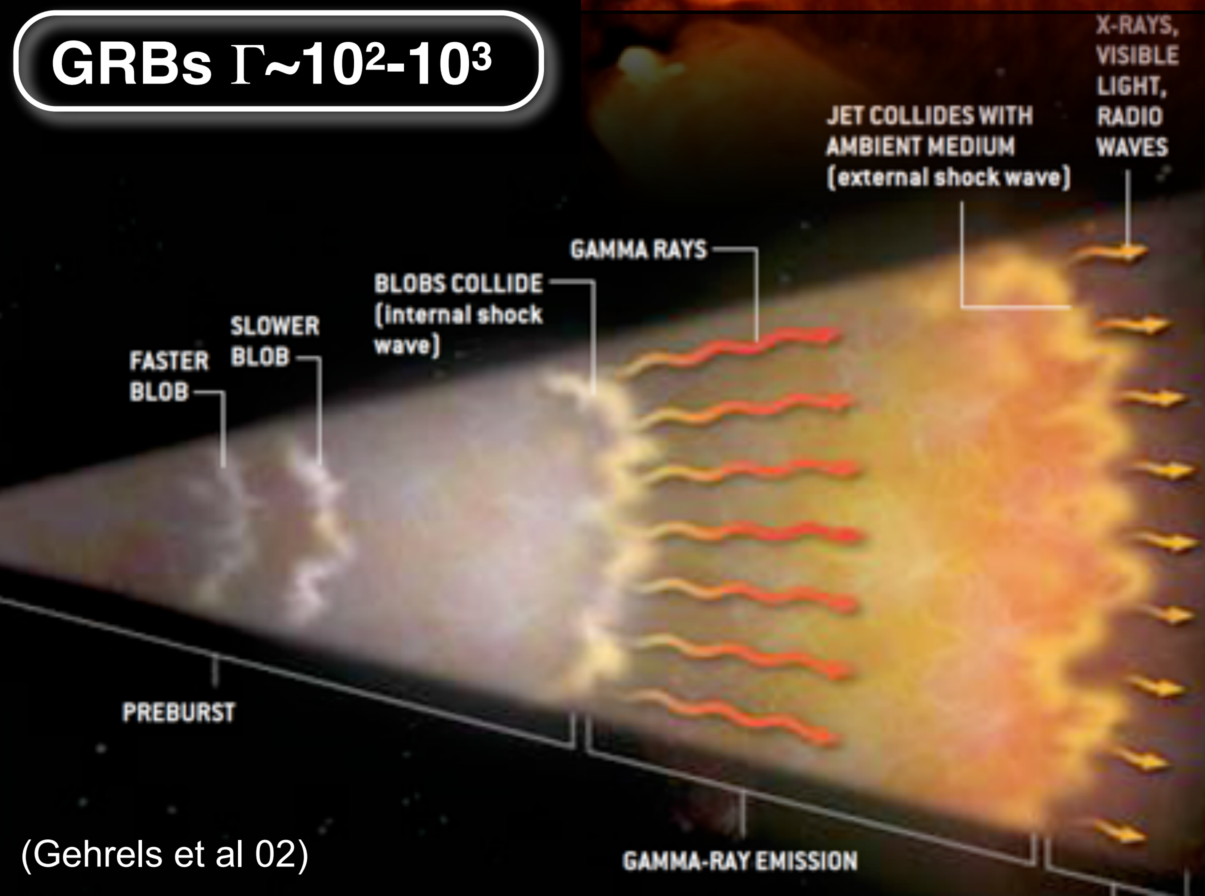

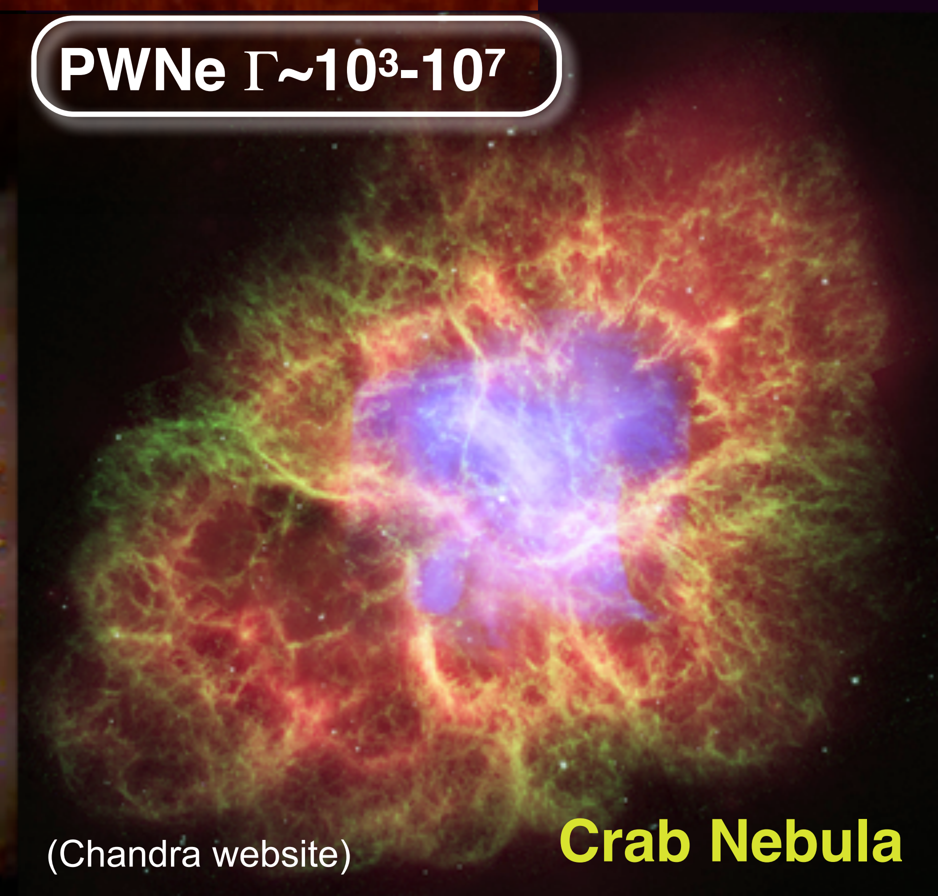

The astrophysical "engine"

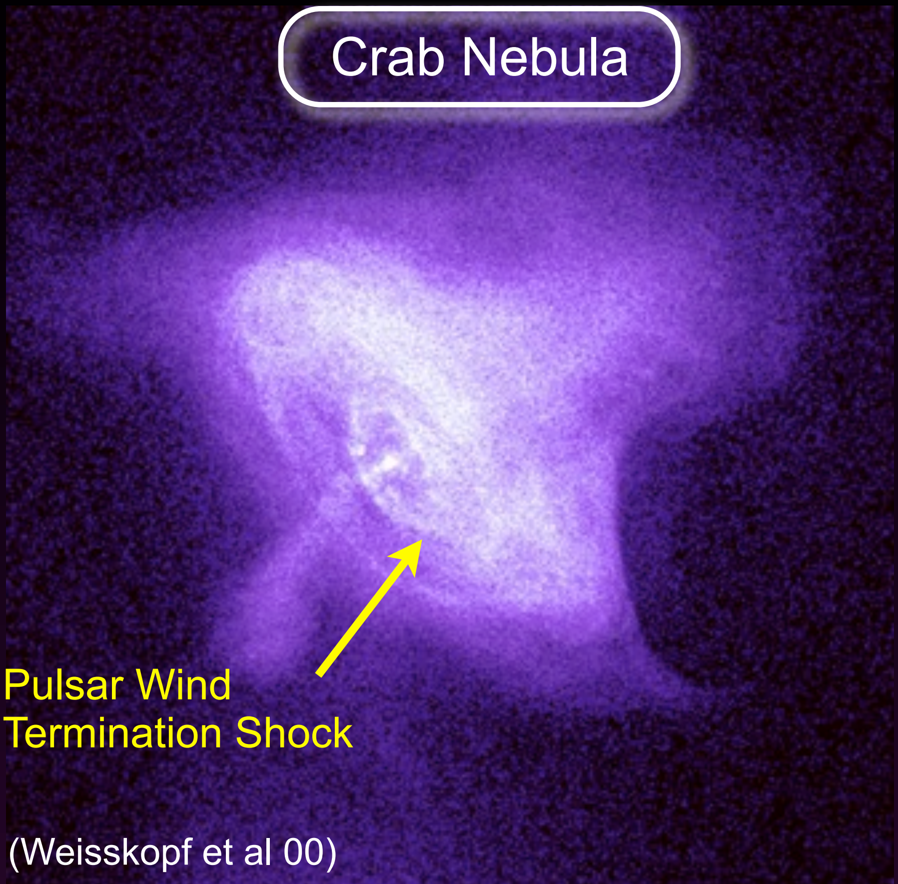

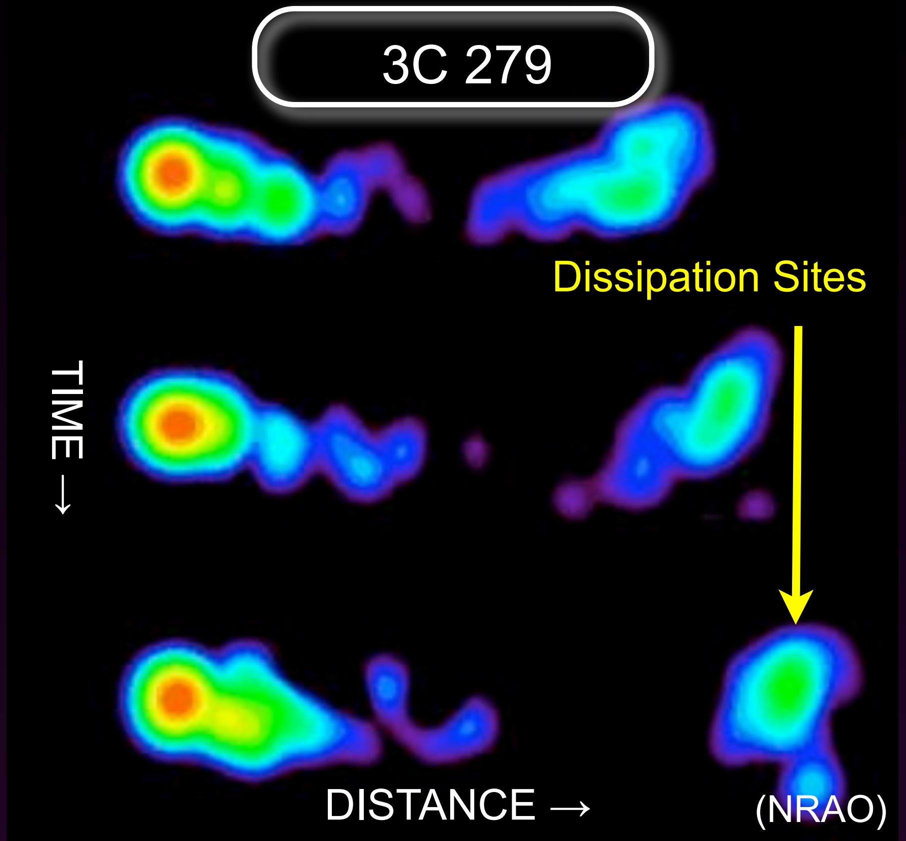

Relativistic astrophysical flows:

- are collisionless. How to dissipate without collisions?
- can vary in composition (pairs or electron-proton)
- can vary in magnetization (magnetic/kinetic energy ratio)

$$\sigma = \frac{B_0^2}{4\pi\gamma_0 n_0 m_p c^2}$$

The astrophysical "exhausts"

Relativistic astrophysical flows are expected to:

- accelerate particles up to non-thermal energies (electrons and UHECRs), with a power-law energy distribution.

- amplify magnetic fields (or generate them from scratch).

- exchange energy between protons and electrons.

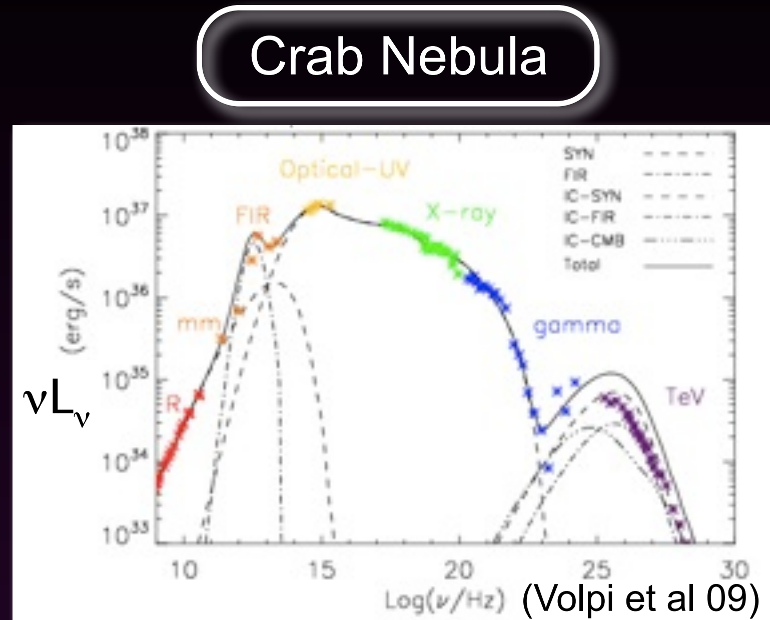

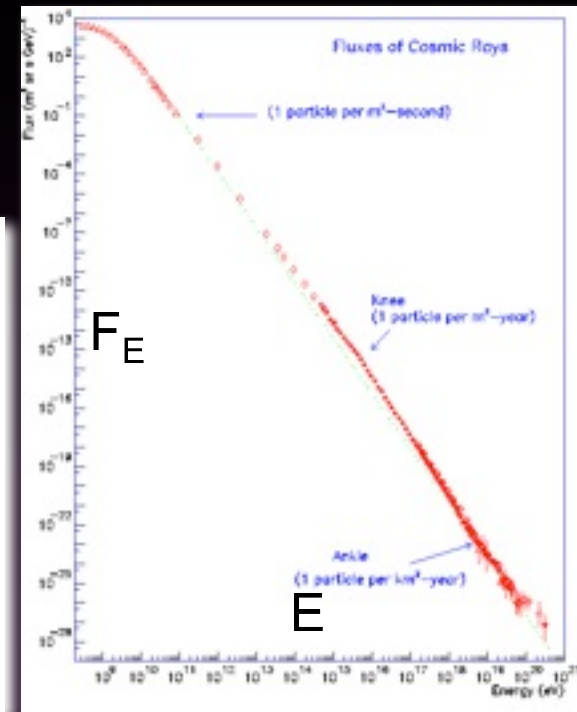

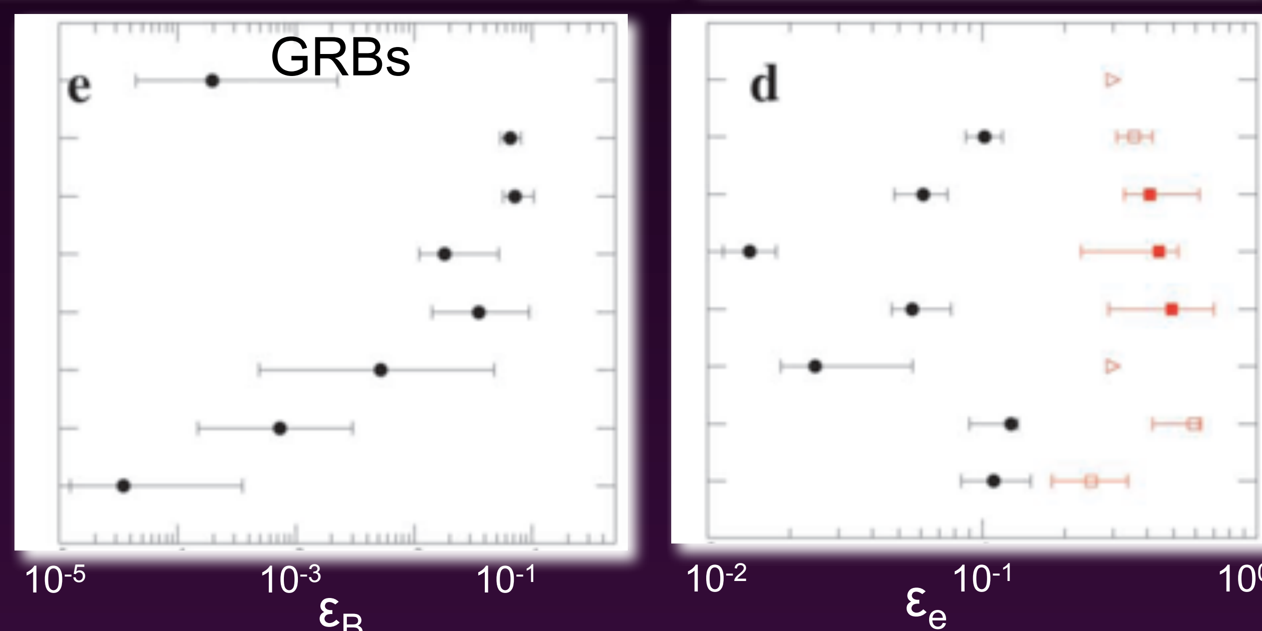

The limitation of phenomenological models

We have no information about (or direct probe of) the nature of the fuel and the mechanics of the engine, but we can only observe the exhausts.

The PIC method

Particle-in-Cell (PIC) method:

1. Particle currents deposited on a grid

2. Electromagnetic fields solved on the grid (Yee's mesh) via Maxwell's equations (Greenwood '04)

3. Lorentz force interpolated to particle locations (Boris pusher)

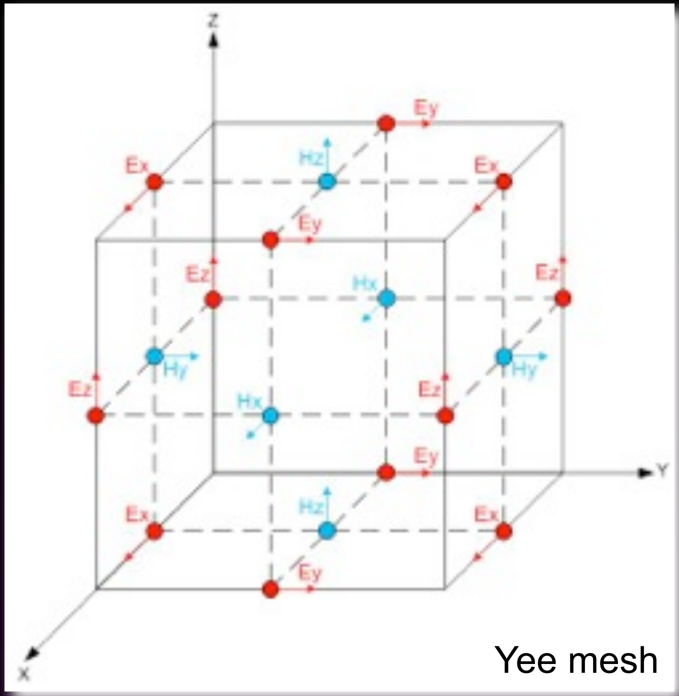

Yee mesh

☺ No approximations, plasma physics at a fundamental level

☹ Tiny length and time scales need to be resolved ➔ huge simulations, limited time coverage

- Relativistic 3D e.m. PIC code TRISTAN-MP (Buneman '93, Spitkovsky '05)

Survey of relativistic shocks

$$\sigma = \frac{B_0^2}{4\pi\gamma_0 n_0 m_p c^2}$$

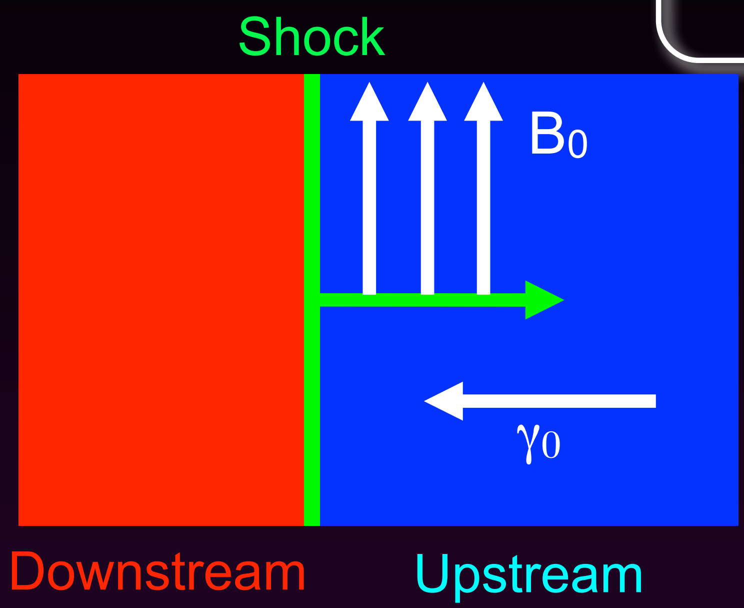

$\sigma=0.1$

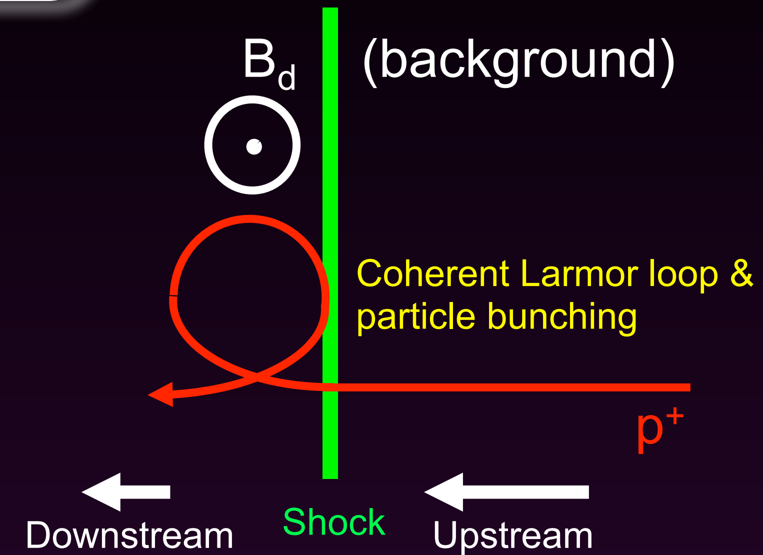

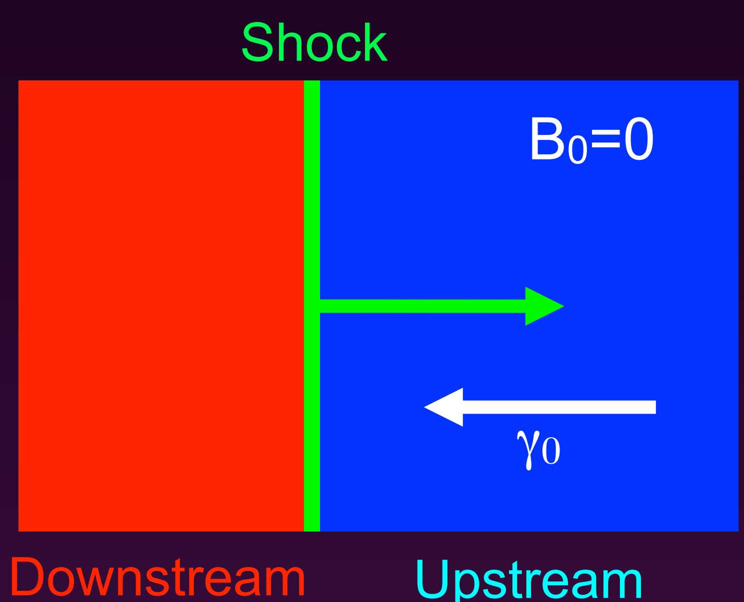

$\sigma=0$

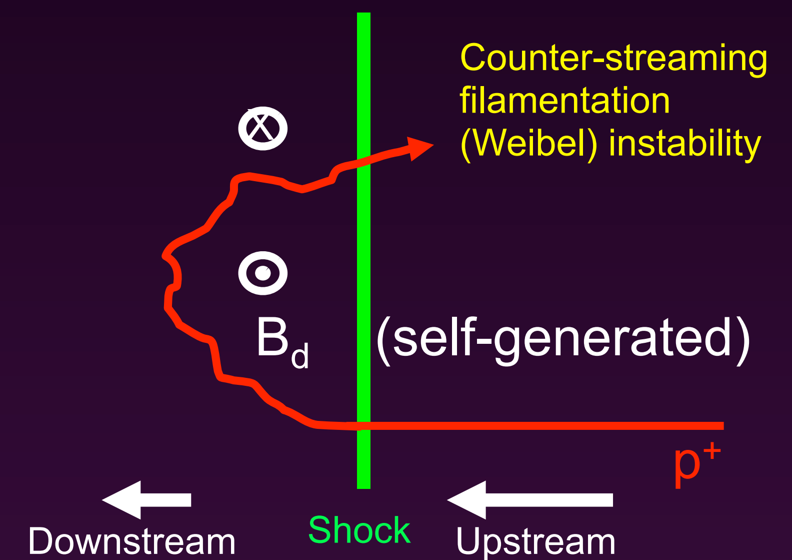

The filamentation (Weibel) instability

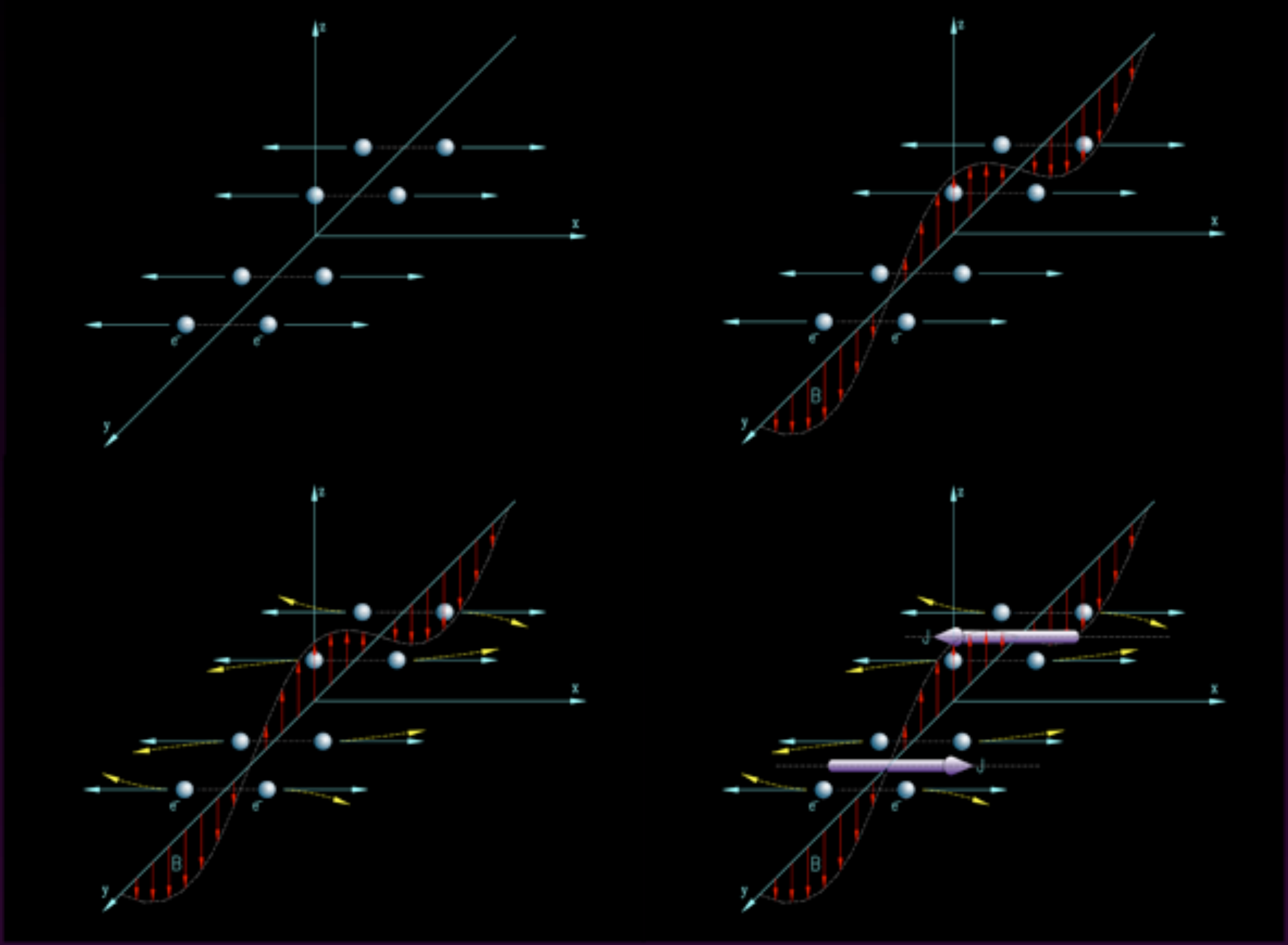

Weibel (1959)
Moiseev & Sagdeev (1963)
Medvedev & Loeb (1999)

Electromagnetic streaming instability that works by filamentation of the plasma
Growth length scale -- skin depth Growth rate -- plasma frequency

$$L \approx c/\omega_{pe} = 10\ \mathrm{km}\ \sqrt{\gamma/\mathrm{n}_0[\mathrm{cm}^{-3}]}$$

$$T \approx 1/\omega_p = 30\ \mu\mathrm{s}\ \sqrt{\gamma/\mathrm{n}_0[\mathrm{cm}^{-3}]}$$

Composition:

1. Electron-positron shocks

2. Electron-proton shocks

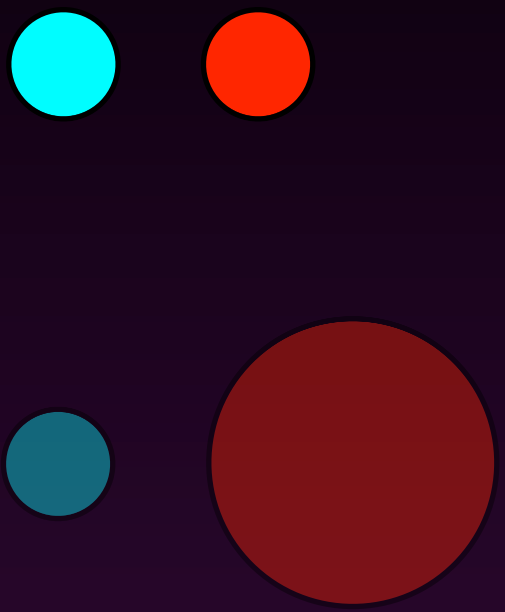

What triggers the shock?

- High-σ shocks: mediated by magnetic reflection

σ=0.1

perp shock

γ_0=15

e^--e^+

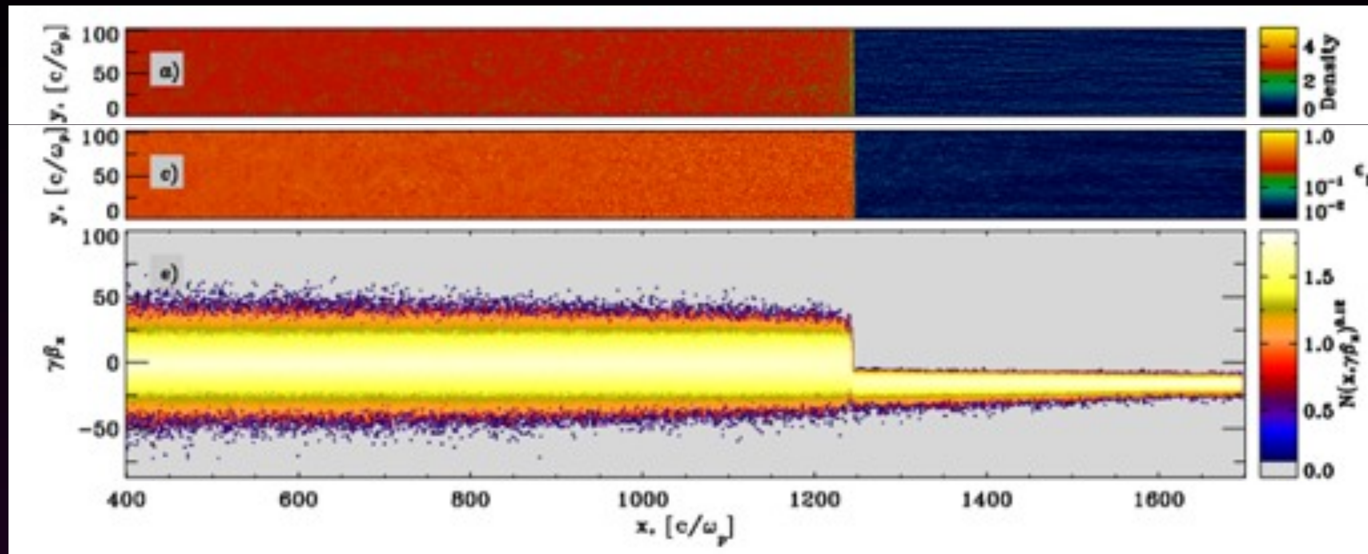

Density

ϵ_B

$\gamma\beta_x$

(LS and Spitkovsky 11)

- Low-σ shocks: mediated by oblique & filamentation instabilities

σ=0

γ_0=15

e^--e^+

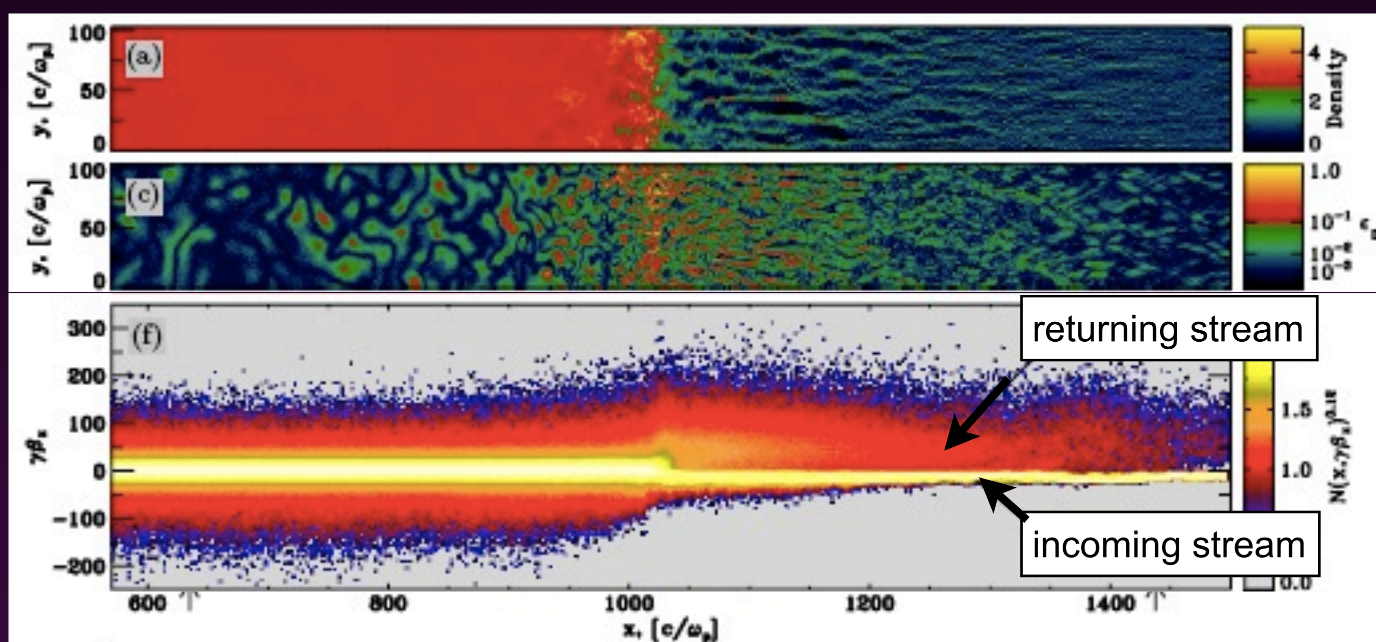

Density

ϵ_B

$\gamma\beta_x$

(Spitkovsky 08)

σ=0 shocks in 3D

Mediated by the filamentation (Weibel) instability, which generates small-scale sub-equipartition magnetic fields.

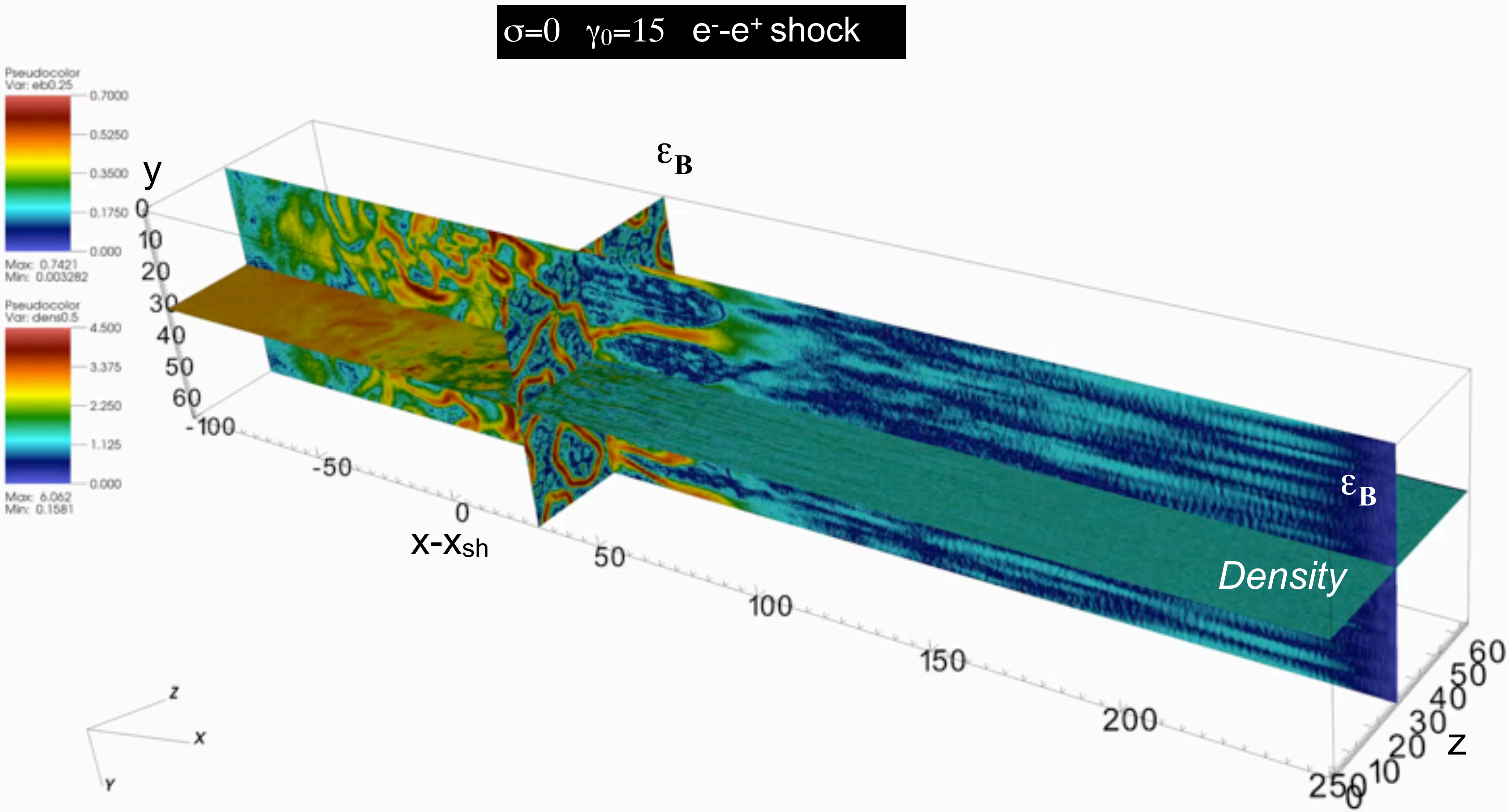

(LS et al. 13)

Turbulence ⇔ Particle acceleration

Returning particles ⇔ Self-generated turbulence

Self-generated turbulence ⇔ Particle acceleration

$\sigma=0.1$ $\theta=90°$ $\gamma_0=15$ e^--e^+ shock

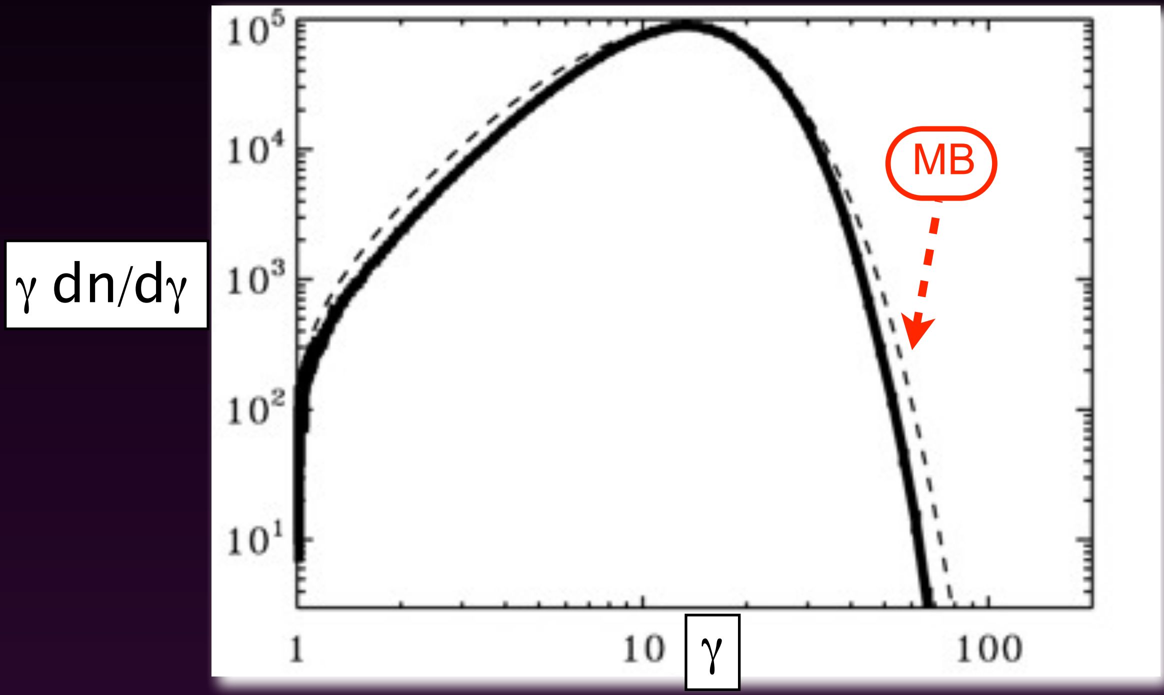

(LS and Spitkovsky 09a)

$\sigma=0$ $\gamma_0=15$ e^--e^+ shock

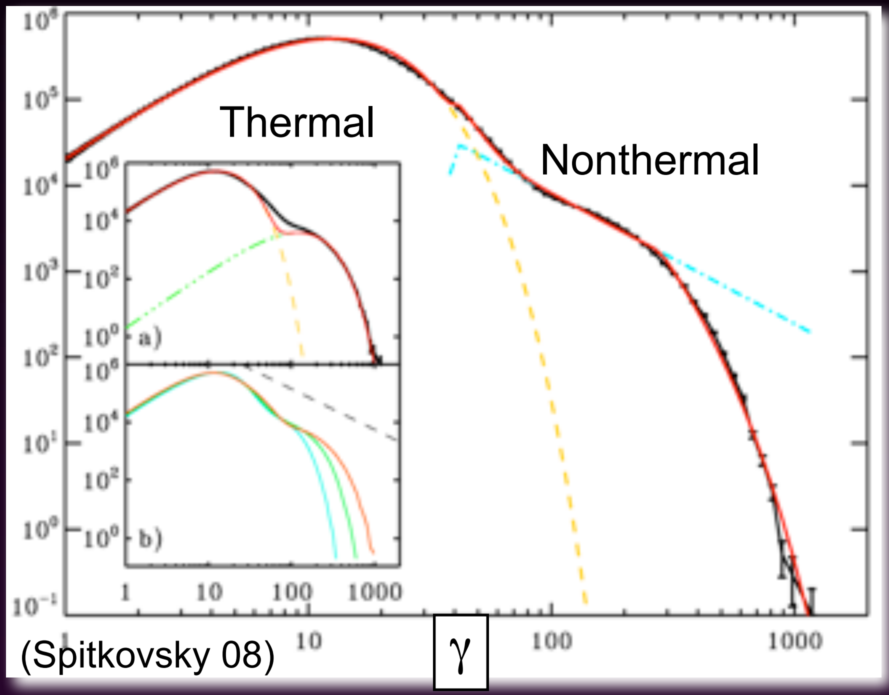

Spectrum fitted by a Maxwellian (entropy generation without collisions)

Spectrum fitted by a Maxwellian + power-law tail. The tail $dn/d\gamma \propto \gamma^{-p}$ has slope $p=2.4\pm0.1$ and contains ~1% of particles and ~10% of energy.

The Fermi process

First-order Fermi process:

Particles bounce between upstream and downstream, gaining energy from the converging flows

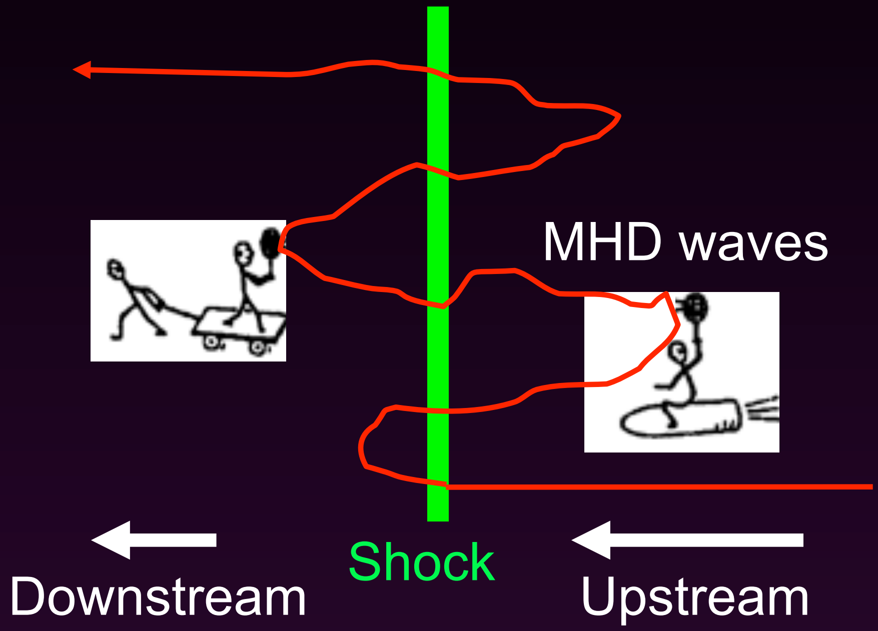

The Fermi process in σ=0 shocks

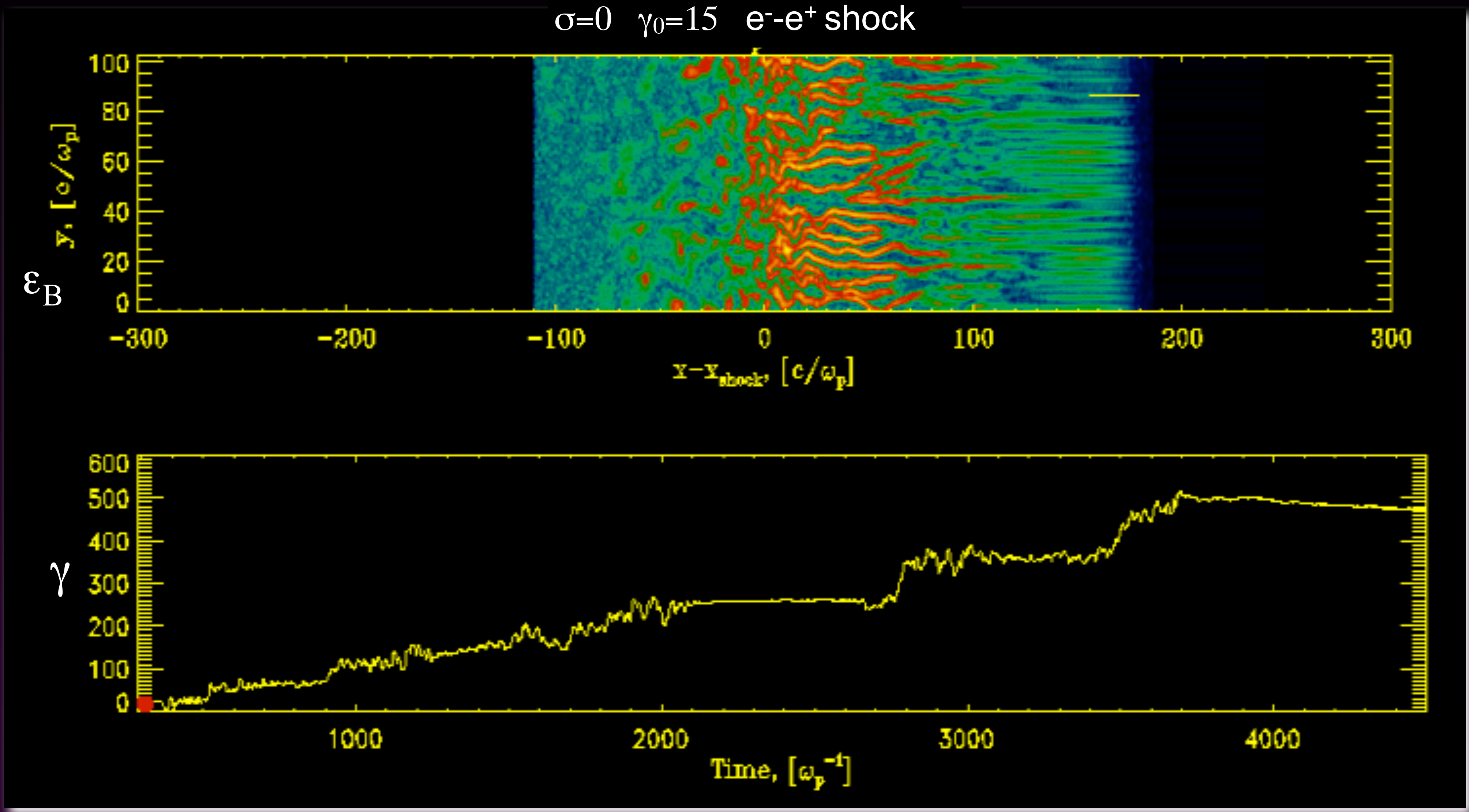

Particle acceleration via the Fermi process in self-generated Weibel turbulence

σ=0 shocks are efficient but slow

The nonthermal tail has slope $p=2.4\pm0.1$ and contains ~1% of particles and ~10% of energy.

By scattering off small-scale Weibel turbulence, the maximum energy grows as $\gamma_{max} \propto t^{1/2}$.

Instead, most models of particle acceleration in shocks assume $\gamma_{max} \propto t$.

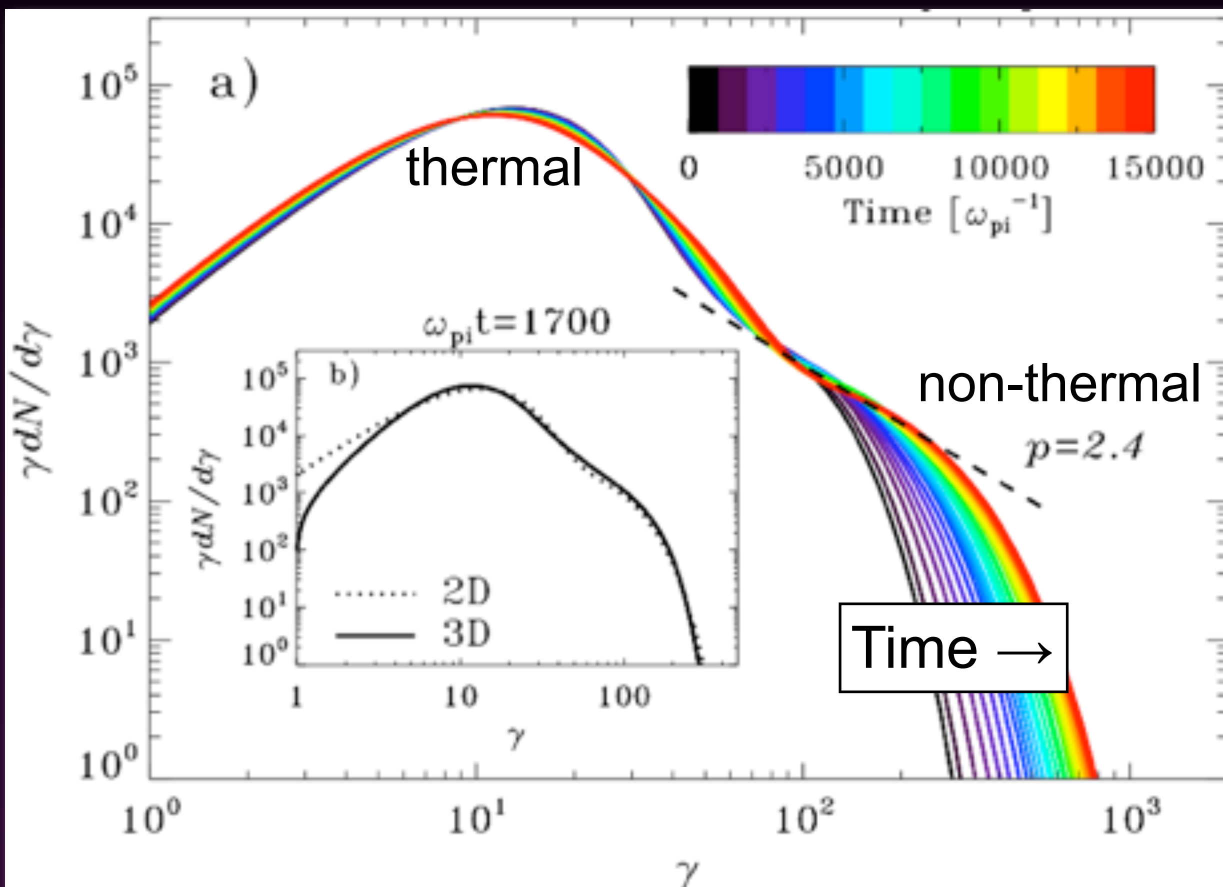

$$\gamma_{max} \simeq 0.5\,\gamma_0\,(\omega_{pi}t)^{1/2}$$

$$D \simeq 4\,c\;c/\omega_{pi}(\varepsilon/\gamma_0 m_i c^2)^2$$

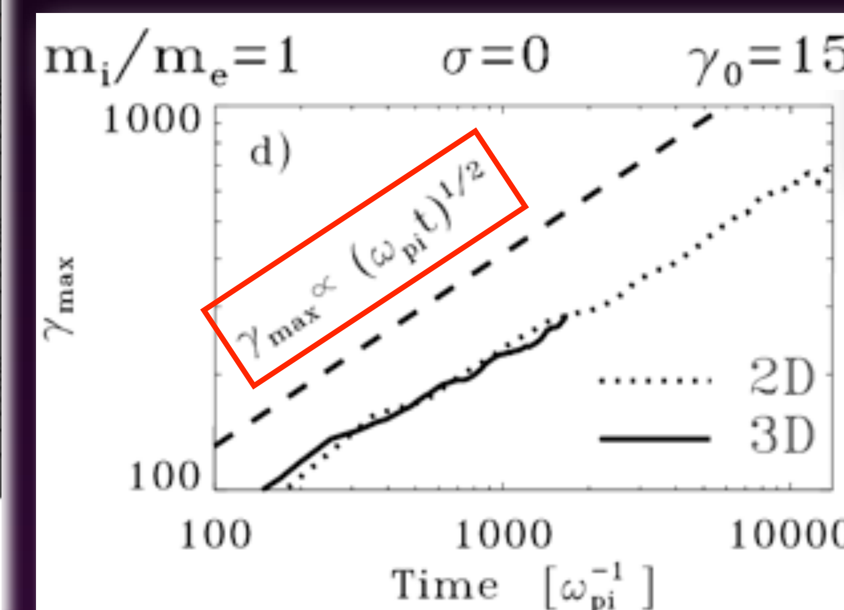

(LS et al. 13)

Conclusions are the same in 2D and 3D

Varying σ: shock structure

e^--e^+ $\gamma_0=15$ shocks

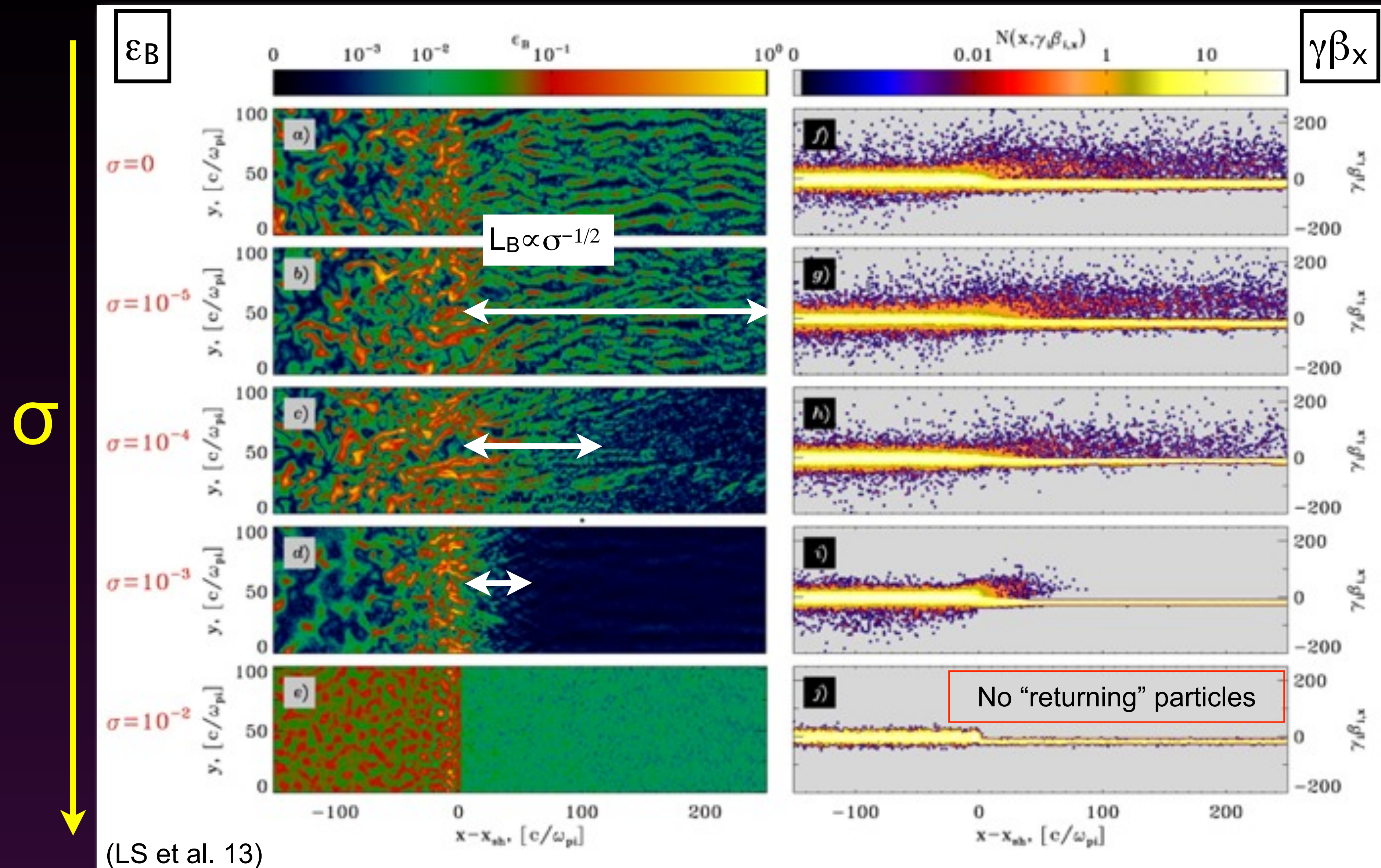

For higher σ, the returning particles are confined closer to the shock by the pre-shock magnetic field, and the Weibel turbulence occupies a smaller region around the shock.

3D shock structure for $\sigma=10^{-3}$

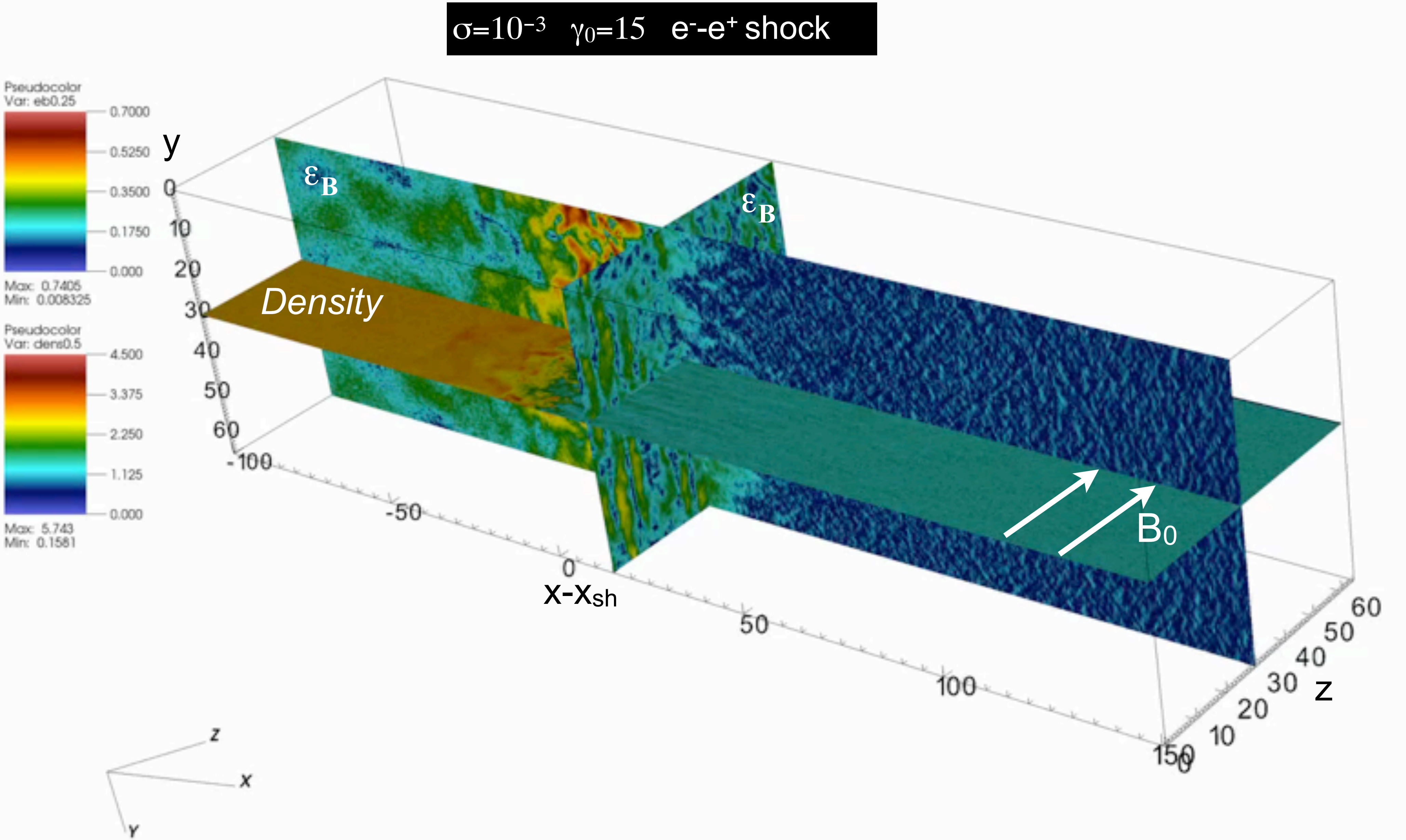

The shock reaches a steady state, and the turbulence stays confined close to the shock.

Spectral evolution for σ=10^{-3}

Thickness of the turbulent layer saturates ⇒ Maximum particle energy saturates

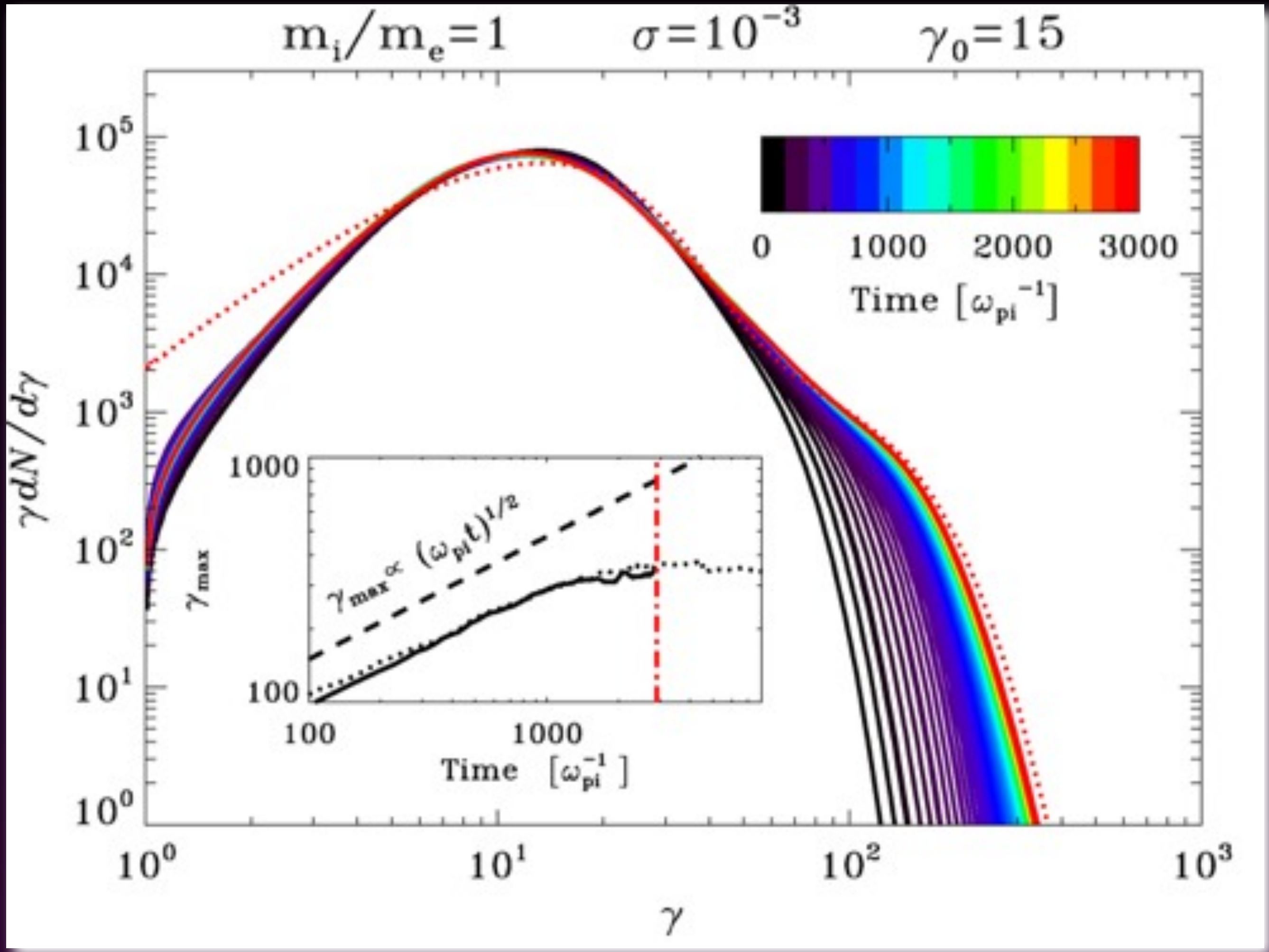

(LS et al. 13)

If $0<\sigma<10^{-3}$, the maximum energy initially grows as $\gamma_{max} \propto t^{1/2}$ but then it saturates, when the shock reaches a steady state.

Energy spectrum vs magnetization

Electron-positron perpendicular shocks are efficient particle accelerators if $\sigma \leq 10^{-3}$.

If $0 < \sigma \leq 10^{-3}$, the Lorentz factor at saturation scales with magnetization as $\gamma_{sat} \propto \sigma^{-1/4}$.

Relativistic perpendicular shocks are poor accelerators if $\sigma > 10^{-3}$.

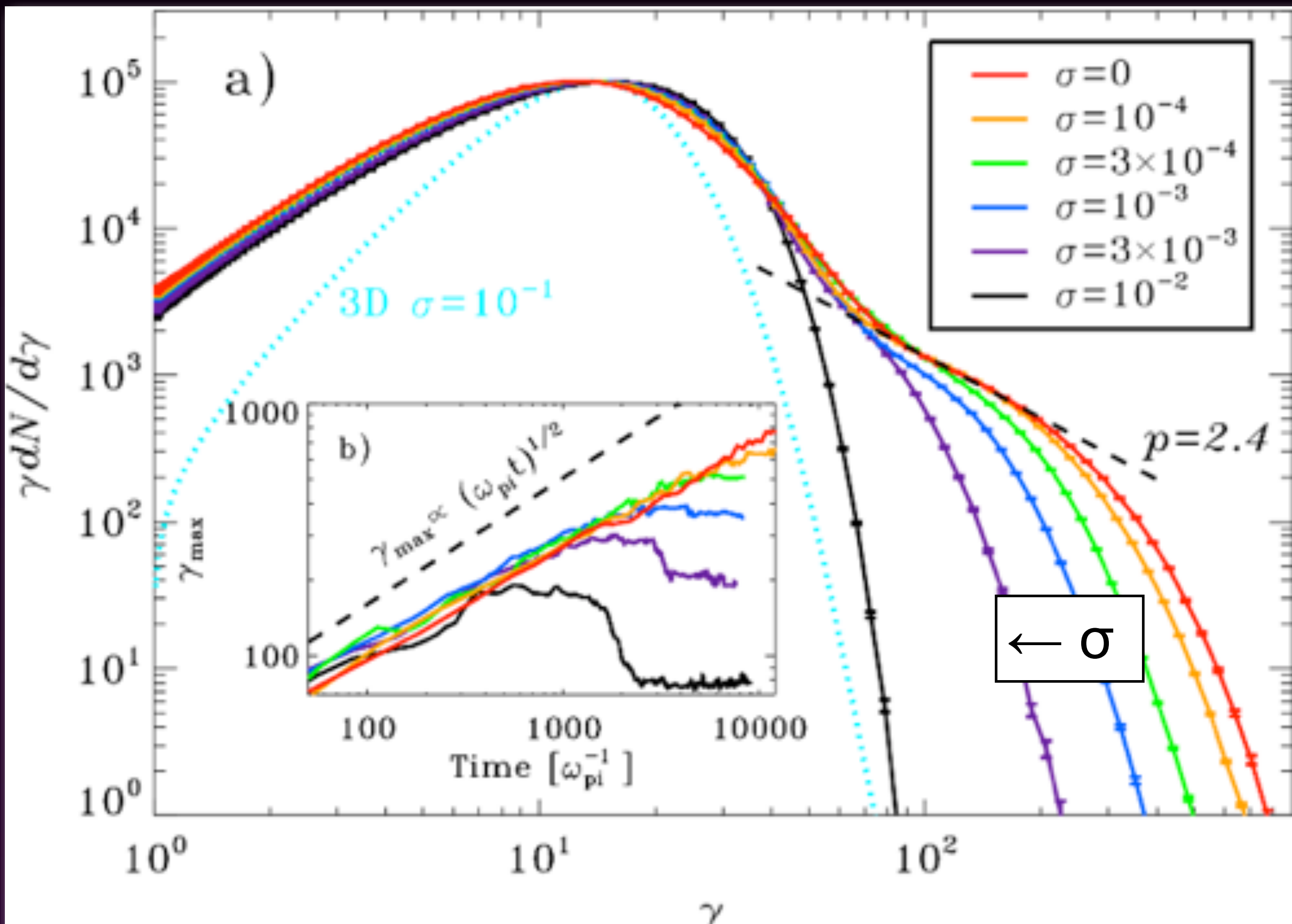

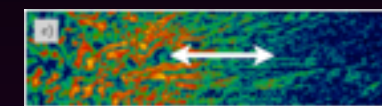

$\gamma_{max} \propto t^{1/2}$ & $L_B \propto \sigma^{-1/2}$

⇓

$$\gamma_{sat} \simeq 4\,\gamma_0\,\sigma^{-1/4}$$

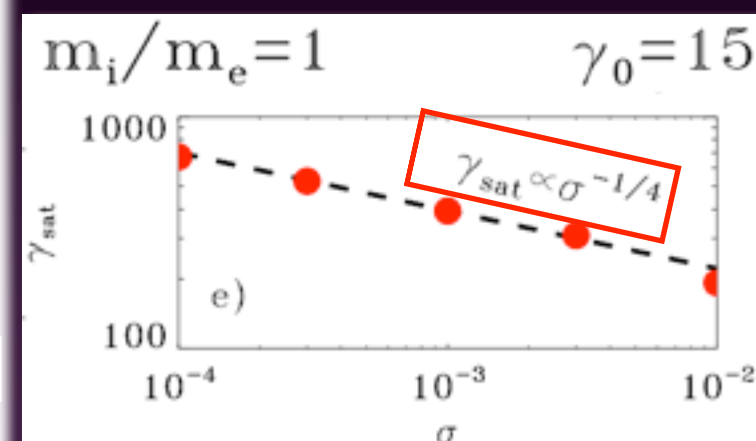

(LS et al. 13)

Composition:

1. Electron-positron shocks

2. Electron-proton shocks

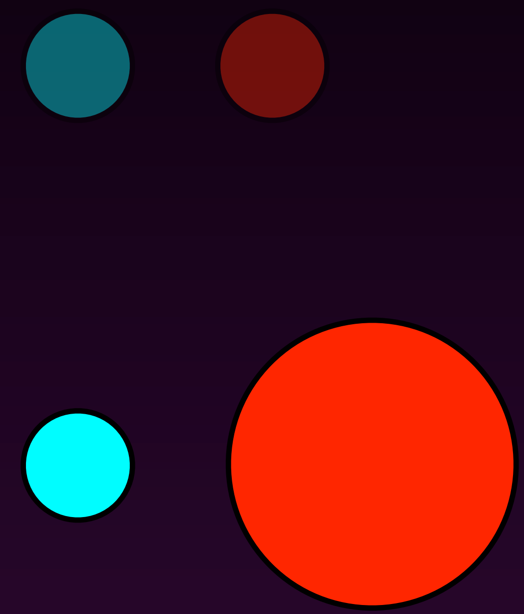

Electron-proton shocks

$m_i/m_e=25$

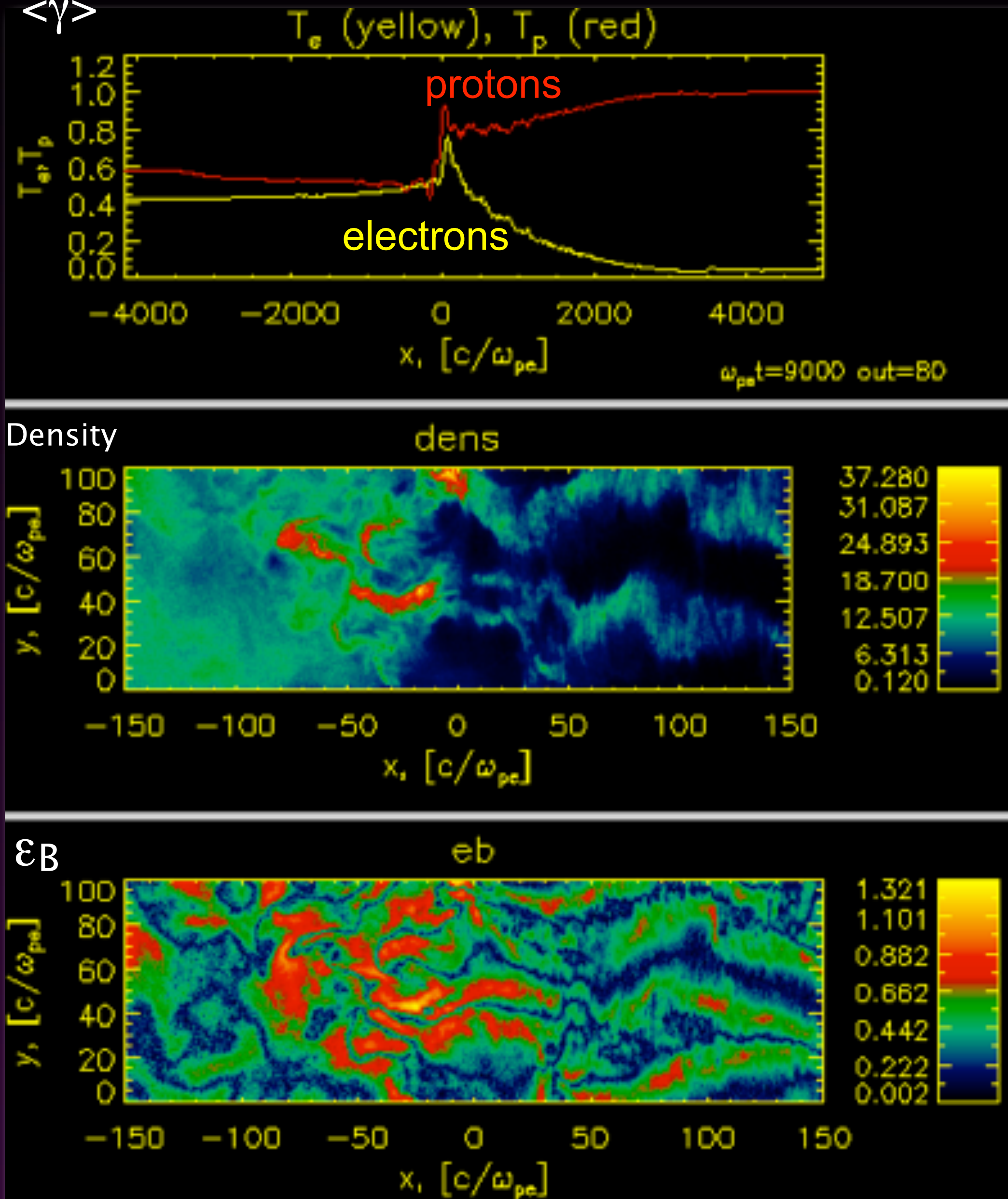

Due to efficient energy transfer ahead of the shock, the energy of the incoming electrons is comparable to the ion bulk energy, and the shock behaves like an electron-positron shock.

$m_i/m_e=1$

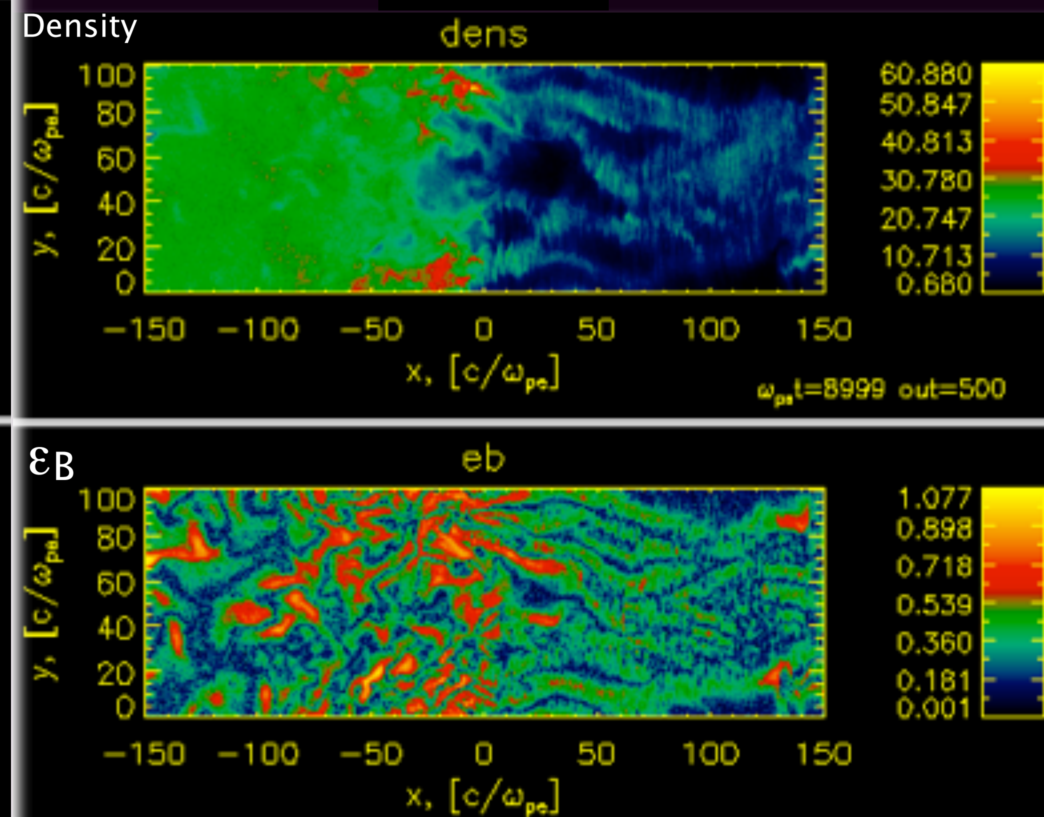

(LS et al. 13)

Electron-proton spectra

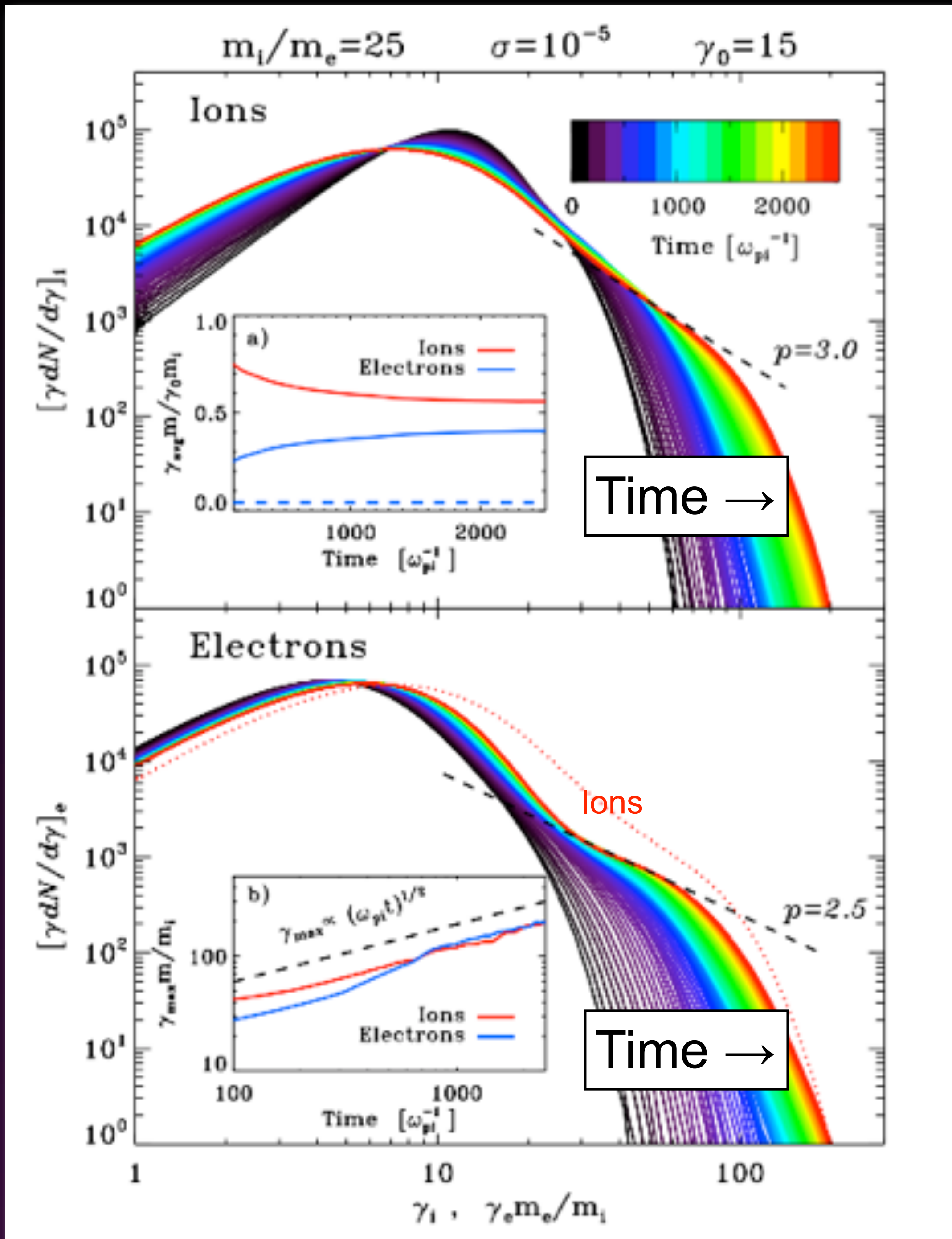

At late times, when electrons and protons are nearly in equipartition, the acceleration efficiency for the two species is the same (~1% by number, ~10% by energy).

The maximum energy of both species grows as $\gamma_{max} \propto t^{1/2}$.

$$\gamma_{max,i} \sim \frac{\gamma_{max,e} m_e}{m_i} \simeq 0.25\, \gamma_0 \,(\omega_{pi} t)^{1/2}$$

$$\gamma_{sat,i} \sim \frac{\gamma_{sat,e} m_e}{m_i} \simeq 2\, \gamma_0\, \sigma^{-1/4}$$

(LS et al. 13)

Dependence on the magnetization

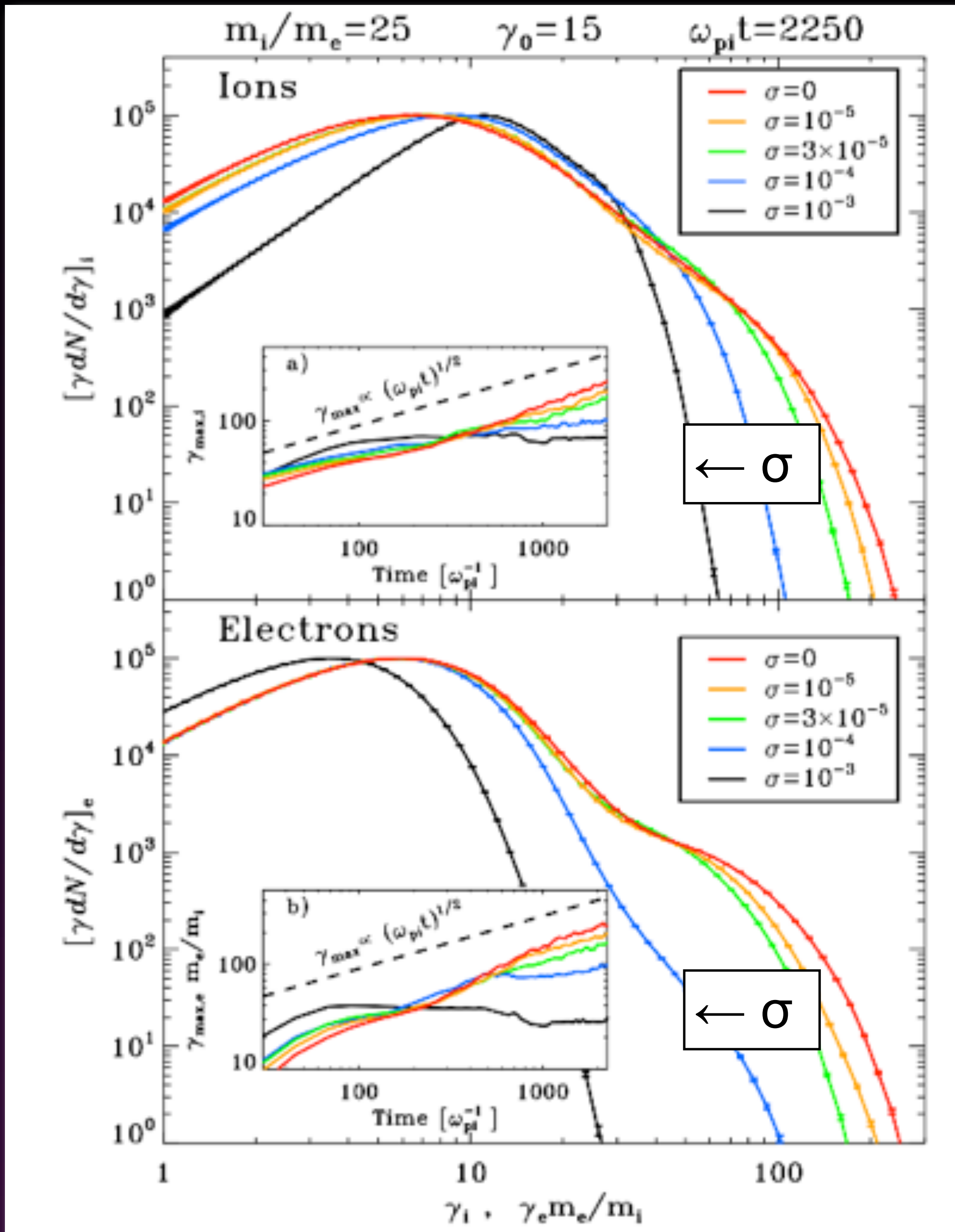

Electrons are efficiently heated regardless of σ, almost in equipartition with the protons.

Magnetized electron-proton perpendicular shocks are efficient particle accelerators only if $\sigma \leq 3\times10^{-5}$.

(LS et al. 13)

Dependence on the mass ratio

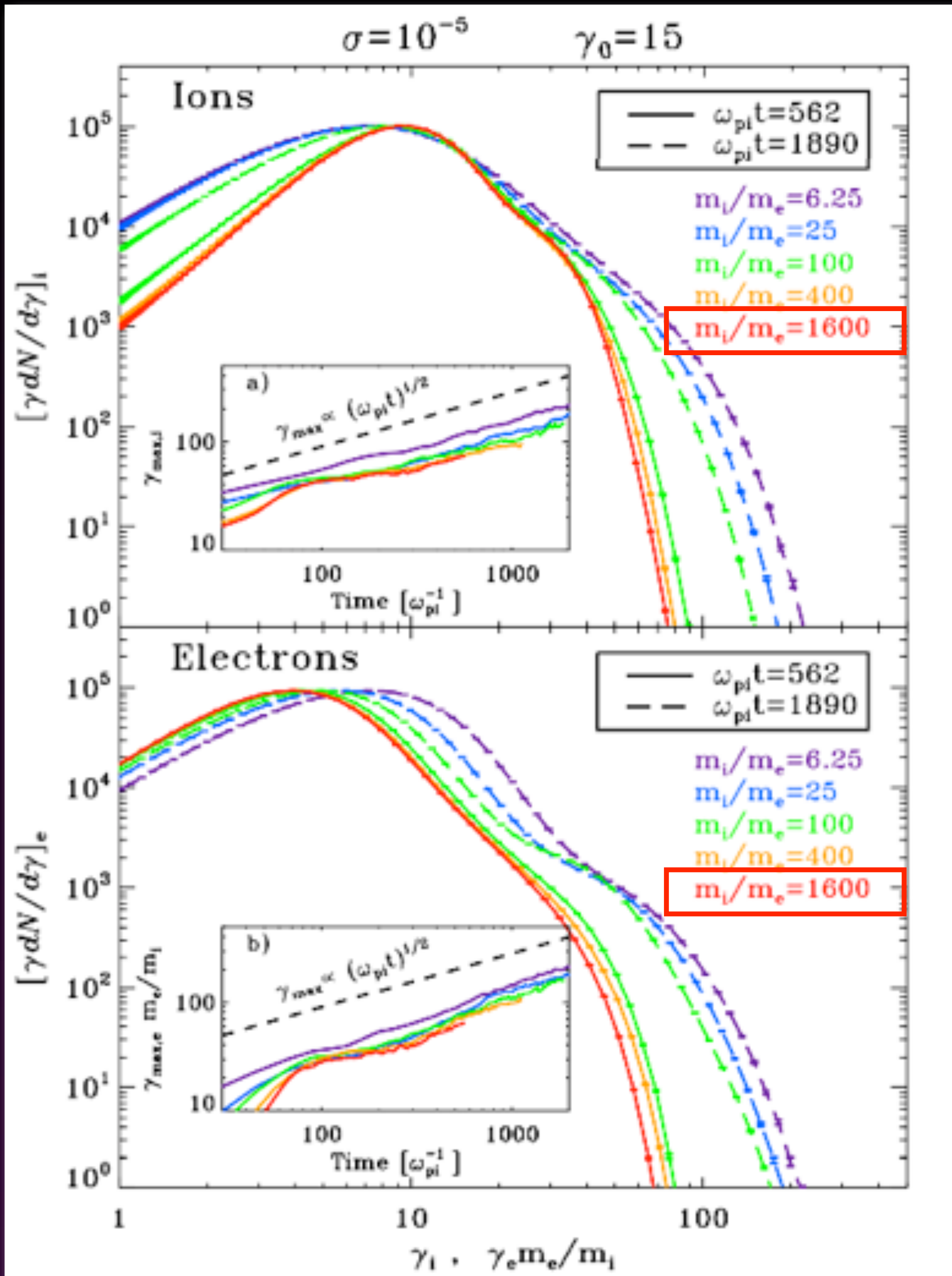

The efficiency of electron heating is independent from the mass ratio.

The acceleration efficiency and the max energy of the accelerated particles are independent from the mass ratio.

(LS et al. 13)

Summary

Fully-kinetic PIC simulations can probe from first principles the microphysics of relativistic astrophysical flows: shock formation, electron heating, particle acceleration

Composition and magnetization are key parameters that determine the shock structure and the efficiency of particle heating/acceleration.

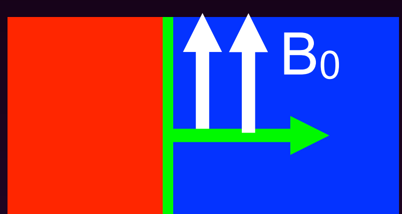

• Strongly magnetized ($\sigma>10^{-3}$) quasi-perpendicular shocks are mediated by magnetic reflection, and are poor particle accelerators. Electrons are heated to equipartition with protons.

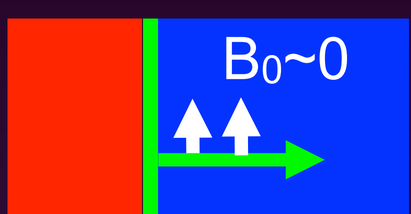

• Weakly magnetized ($\sigma<10^{-3}$) shocks are mediated by counter-streaming instabilities, and are efficient particle accelerators (~1% by number, ~10% by energy). The maximum energy grows as $\gamma_{max}\propto t^{1/2}$ until it saturates at $\gamma_{sat}\propto\sigma^{-1/4}$.